

# Spectral reproduction from scene to hardcopy

## Part I – Multi-spectral acquisition and spectral estimation using a Trichromatic Digital Camera System associated with absorption filters

*Francisco H. Imai*  
*Munsell Color Science Laboratory, Rochester Institute of Technology*

### Abstract

This report summarizes a research performed to evaluate the accuracy of a new multi-spectral acquisition system based on *a priori* spectral analysis followed by wide-band capture combining trichromatic camera and absorption filters. This report will be focused on comparing the performance of the new method with the more conventionally used narrow band multi-spectral acquisition that employs interference filters. This report will also show the potentiality of this method demonstrating that the information generated using an *a priori* analysis performed using a general target can be used in the spectral estimation of a different target.

### Introduction

The traditional techniques of image capture used to archive artwork in most of the museums of the world rely on conventional photographic processes. Photography has the advantages of high-resolution and optimal luminance (tone) reproduction and the disadvantage of poor color accuracy. The exception is the VASARI imaging system developed at the National Gallery, UK which employs a seven-channel multi-spectral 12 bit digital camera attached to a scanning device that traverses across the painting.<sup>1</sup> After appropriate signal and spatial processing, 20K x 20K 10-bit L\*, 11-bit a\* and b\* encoded images result. The National Gallery has been very successful in developing colorimetric image archives and using them to provide the European community with accurate color reproductions in both soft-copy and hard-copy forms under a defined set of illuminating and viewing conditions (i.e., colorimetric color reproduction).

We have an interest in drawing upon the European experiences and making some enhancements. We would like to define images spectrally and use the spectral information to provide printed color reproductions that are close spectral matches to the original objects producing high-quality color matching under different illuminations and observers. The advantages of spectral systems have been summarized by Berns<sup>2</sup> and Hardeberg et al.<sup>3</sup> Technical issues concerned with multi-spectral image acquisition have been exhaustively studied.<sup>4-9</sup> In particular, König and Praefcke<sup>10</sup> analyzed practical problems of designing and operating a multi-spectral scanner using a set of narrow-band interference filters and a monochrome CCD camera, the most common configuration for multi-spectral image capture. When using interference filters for image acquisition, a major problem is caused by the transmittance characteristic of the filters that depends on the angle of incidence. For example, in order to image a painting with horizontal dimensions of 1 meter with a distance of 2 meters between the painting and the filter, there is angle of incidence  $\sim 14^\circ$  for points in the extremities. Simulations<sup>10</sup> have shown that this causes color differences of  $2 E^*_{ab}$  units in relation to the image obtained at  $0^\circ$  angle of incidence. Another problem is that the surfaces of the interference filters are not exactly coplanar resulting in spatial shift and distortion of the captured image. We also need to consider that there are inter-reflections caused by reflections between the spectral filters and the original image, and between the interference filters and the camera lens. These technical problems make it unrealistic and impractical for image acquisition using interference filters in museums without a considerable degree of expertise in multi-spectral imaging.

We believe that a conventional trichromatic digital camera combined with absorption filters can provide an alternative way to capture multi-spectral images. The spectral reflectance of each pixel of the image can be calculated by the camera signals using linear methods. It makes the image acquisition easier and with relatively low cost since the performance-cost relation of commercial digital cameras has increased rapidly.

In a previous technical report<sup>11</sup> the digitizing system using a trichromatic IBM PRO\3000 Digital Camera System (4,920 by 3,072 pixels, 12 bits quantization, copy stand with good geometric stability and possibility to operate as a monochromatic digital camera)<sup>12, 13</sup> and a set of Kodak Wratten<sup>14</sup> absorption filters shown in Figure 1 were fully characterized and some preliminary experiments showed the feasibility of using this method to reconstruct spectral reflectance from a multiple-of-three set of digital counts. The a trichromatic digital camera with good colorimetric performance, sufficient resolution (4,920 by 3,072 pixels), 12 bits quantization and geometric stability for imaging is used



**Figure 1.** IBM PRO\3000 Digital Camera System head and Kodak Wratten absorption filter with the filter holder.

As a resulting of the imaging using this system we have a set of images as shown in Figure 2.

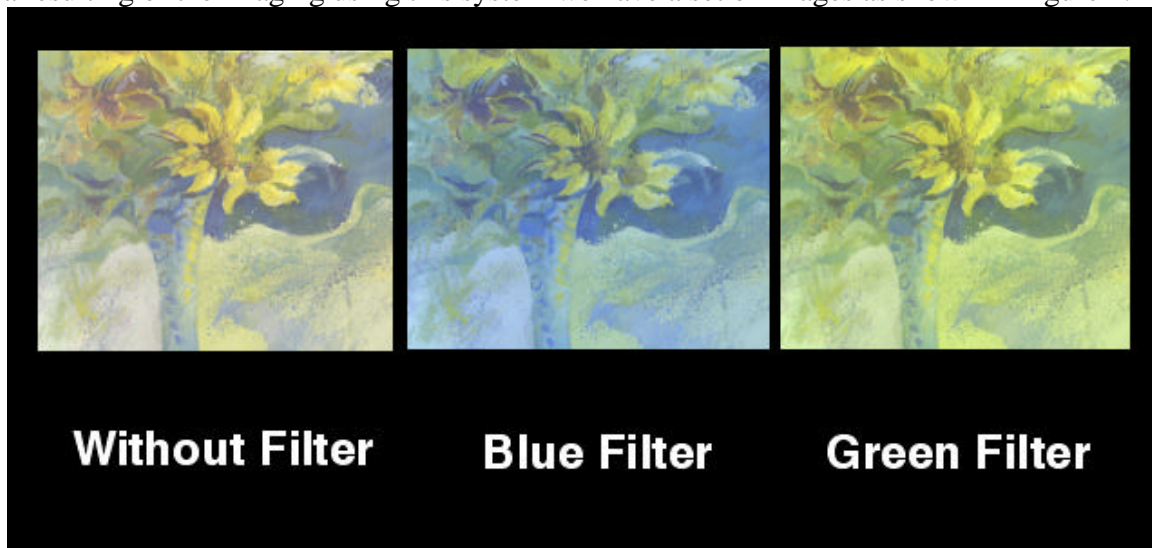


**Figure 2.** Image of painting digitized by a trichromatic camera and a set of two filters.

In order to relate the digital counts to spectral reflectance, a linear method based on camera modeling was applied with elements shown in Figure 3. The spectral radiance,  $\mathbf{S}$ , of the illuminant, as well as the spectral sensitivities,  $\mathbf{D}$ , of the camera, the transmittances,  $\mathbf{F}$ , of the filters and the spectral reflectance,  $\mathbf{r}$ , of color patches are measured and the digital counts,  $\mathbf{Dc}$ , were extracted from the imaged patches.

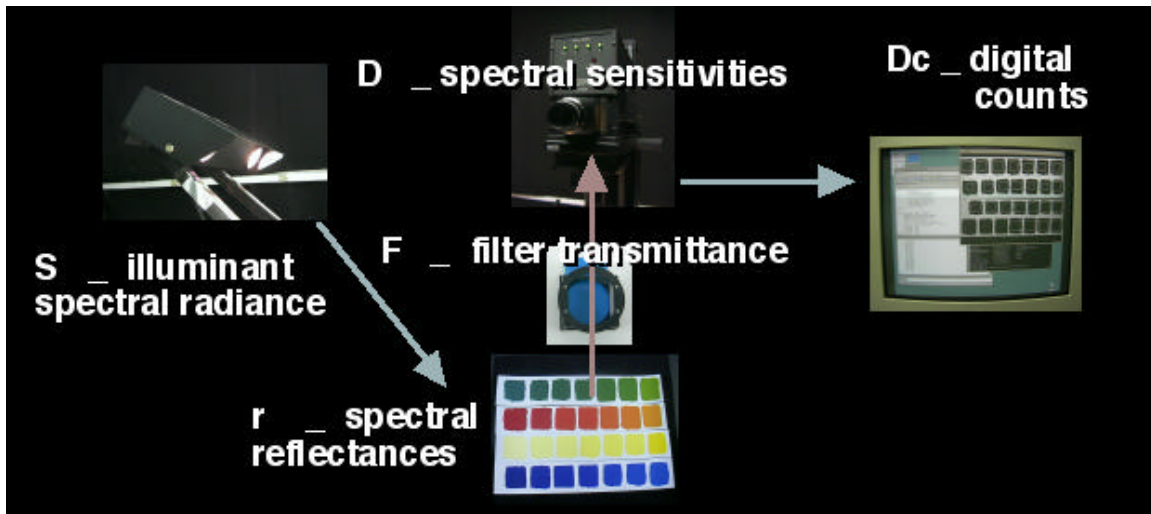


**Figure 3.** Schematic diagram showing the elements of camera modeling used in the experiments.

The spectral reflectance of each pixel of a painting could be estimated using *a priori* spectral analysis with direct measurement and imaging of color patches to establish a relationship between the digital counts and spectral reflectance as shown in Figure 4.

]

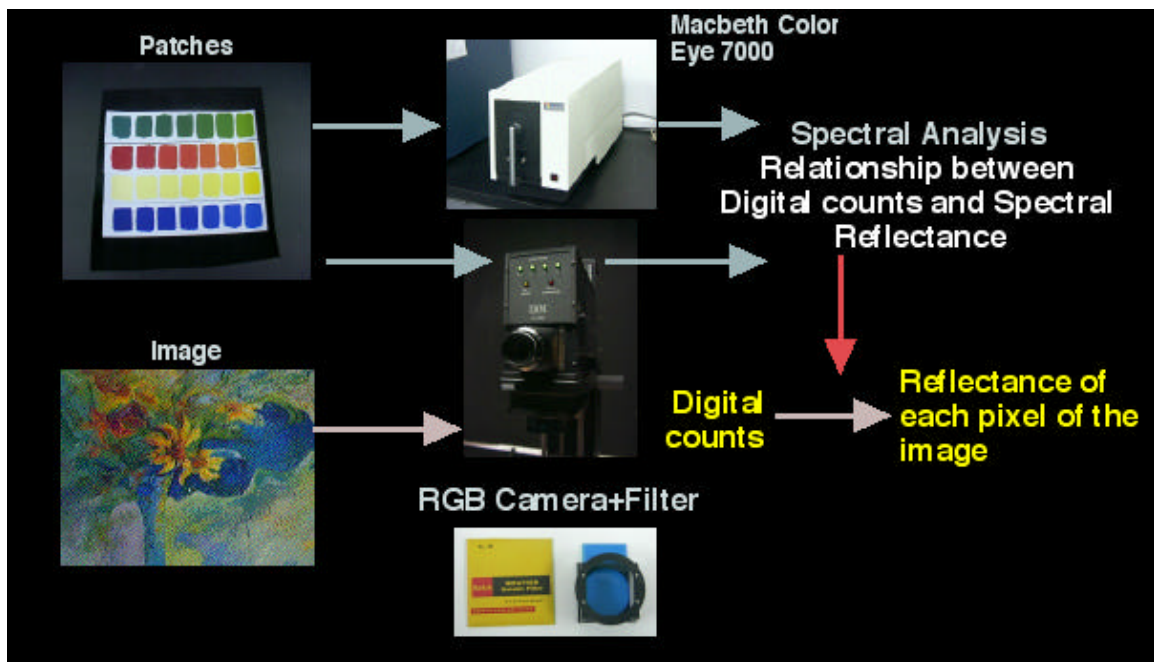


**Figure 4.** Schematic diagram of the method used to estimate the spectral reflectance of each pixel of an image using a trichromatic camera and a set of absorption filters.

### Linear method

One can model multi-spectral image acquisition using matrix-vector notation.<sup>15</sup> Expressing the sampled illumination spectral power distribution as

$$\mathbf{S} = \begin{pmatrix} s_1 & & & 0 \\ & s_2 & & \\ & & \ddots & \\ 0 & & & s_n \end{pmatrix}, \quad (1)$$

and the object spectral reflectance as  $\mathbf{r}=(r_1, r_2, \dots r_n)^T$ , where the index indicates the set of  $n$  wavelengths over the visible range and  $\tau$  the transpose matrix, representing the transmittance characteristics of the  $m$  filters as columns of  $\mathbf{F}$

$$\mathbf{F} = \begin{pmatrix} f_{1,1} & f_{1,2} & \dots & f_{1,m} \\ \vdots & \vdots & \dots & \vdots \\ f_{n,1} & f_{n,2} & \dots & f_{n,m} \end{pmatrix} \quad (2)$$

and the spectral sensitivity of the detector as

$$\mathbf{D} = \begin{pmatrix} d_1 & & & 0 \\ & d_2 & & \\ & & \ddots & \\ 0 & & & d_n \end{pmatrix}, \quad (3)$$

then the captured image is given by  $\mathbf{D}_c=(\mathbf{DF})^T\mathbf{S}\mathbf{r}$ , where  $\mathbf{D}_c$  represents the digital counts, and the color vector can be represented as  $\mathbf{c}=\mathbf{A}\mathbf{t}=(X, Y, Z)^T$  where  $X, Y, Z$  are the CIE tristimulus values. The CIELAB  $L^*, a^*, b^*$  are given by the non-linear transformation, where  $(X, Y, Z) = L^*, a^*, b^*$ .

If the spectral reflectance is sampled in the range of 400 nm to 700 nm wavelength in 10 nm intervals we have 31 samples. Ideally we should have 31 signals to reconstruct the spectral reflectance. However, it is possible to decrease the dimensionality of the problem by performing principal component analysis on the spectral samples. Given a sample population of spectral reflectances, it is possible to identify a small set of underlying basis functions whose linear combinations can be used to approximate and reconstruct members of the populations.<sup>15-19</sup> Then the reconstructed sample  $\hat{r}_i$  is given by  $\hat{r}_i = \sum_{i=1}^p \mathbf{v}_i$ , where  $\mathbf{v}_i = (\mathbf{e}_1 \ \mathbf{e}_2 \ \dots \ \mathbf{e}_p)$  are the set of the eigenvectors (principal components) used for the estimation and the coefficients (eigenvalues) associated with the eigenvectors are  $\mathbf{a}_i = (\mathbf{a}_1 \ \mathbf{a}_2 \ \dots \ \mathbf{a}_p)^T$  where the index  $p \leq n$ , and where  $n$  is the number of samples used to perform *a priori* principal component analysis. When the eigenvalues are arranged in descending order the fraction of variance explained by the first corresponding  $p$  vectors is

$$\mathbf{v}_p = \frac{\sum_{i=1}^p \mathbf{a}_i}{\sum_{i=1}^n \mathbf{a}_i}. \quad (4)$$

In this linear method, a set of spectral reflectances  $\mathbf{r}$  is measured and then a set of eigenvectors, who explain typically more than 99.9% of the original sample, is calculated by principal component analysis. Then, the set of eigenvalues,  $\mathbf{a}_i$ , is calculated by  $\mathbf{a}_i = \mathbf{r}^T \mathbf{r}$ , where  $\mathbf{r}^T$  denotes the transpose of the matrix. We know that the set of digital counts corresponding to the spectral samples can be calculated by the equation  $\mathbf{D}_c=(\mathbf{DF})^T\mathbf{S}\mathbf{r}$ . A relationship between digital counts and eigenvalues can be established by the equation

$$\mathbf{A} = \mathbf{Dc}^T [\mathbf{DcDc}^T]^{-1} \quad (5)$$

The matrix  $\mathbf{A}$  can be used to calculate the eigenvalues  $\mathbf{a}_i$  from digital counts to reconstruct the spectral reflectance. Here, it is important to notice that the number of channels should equals the number of eigenvectors used in the system.

## Experimental

### I) Measurement of samples

Three targets were used in this experimental part. The GretagMacbeth ColorChecker rendition chart shown in Figure 5a and two different sets of painted patches were used in the experiment. One set of painting patches shown in Figure 5b was generated using a mixture of GALERIA acrylic paints produced by Winsor & Newton (Cadmium Red Hue, Permanent Green Deep, Ultramarine, Cerulean Blue Hue, Permanent Magenta, Cadmium Yellow Medium Hue). The acrylic painted patches shown in Figure 5c were made with mixtures of two and three colorants generating 218 patches. The other set of painted patches were generated using post-color paints (Cerulean Blue and Rose Violet made by Sakura, Ultramarine, Permanent Yellow, Sap Green and Black made by Pentel). The post-color painted patches were made with mixtures of two colorants generating 105 patches. The post-color patches were coated with Krylon Kamar Varnish that is a non-yellowing protection.



**Figure 5a.** GretagMacbeth ColorChecker.



**Figure 5b.** Set of the 218 acrylic painted patches.

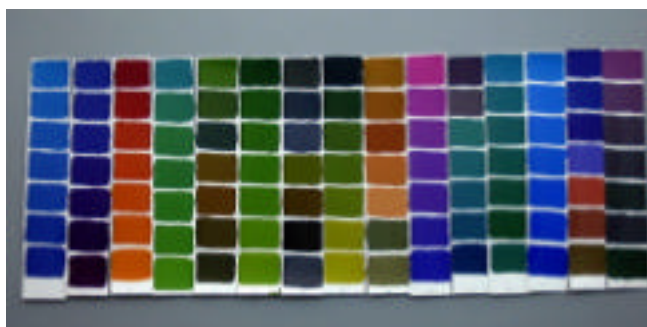


**Figure 5c.** Set of the 105 poster-color painted patches

The spectral reflectances of the Macbeth ColorChecker were measured in wavelength intervals of 10 nm from 400nm to 700nm using the Macbeth ColorEye 7000 spectrophotometer with integration sphere (specular included, UV excluded); the painted patches were measured using GRETAG SPM60 45/0 spectrophotometer.

The distribution in  $a^* \times b^*$  space of the GretagMacbeth ColorChecker for D50 illuminant and  $2^\circ$  observer is shown in Figure 6.

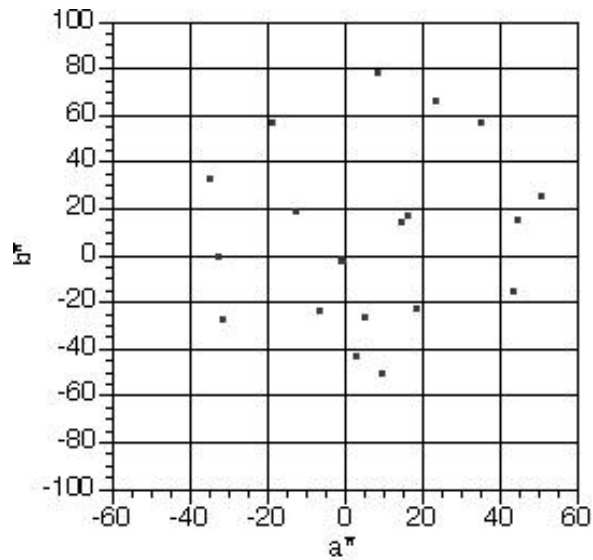


**Figure 6a.**  $a^*b^*$  plot for Macbeth ColorChecker (D50 illuminant,  $2^\circ$  observer).

The  $a^* \times b^*$  distribution for D50 illuminant and  $2^\circ$  observer for the acrylic painted patches is shown in Figures 6b.

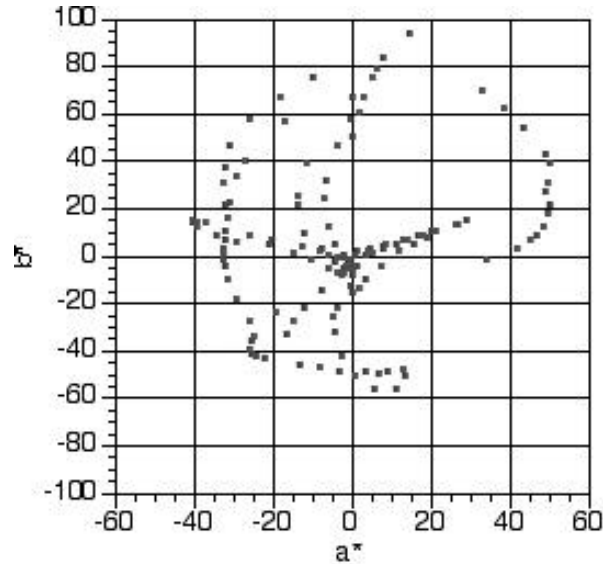


**Figure 6b.**  $a^*b^*$  plot for the acrylic painted patches (D50 illuminant,  $2^\circ$  observer)

The  $a^* \times b^*$  distribution for D50 illuminant and  $2^\circ$  observer for the poster-color painted patches is shown in Figures 6c.

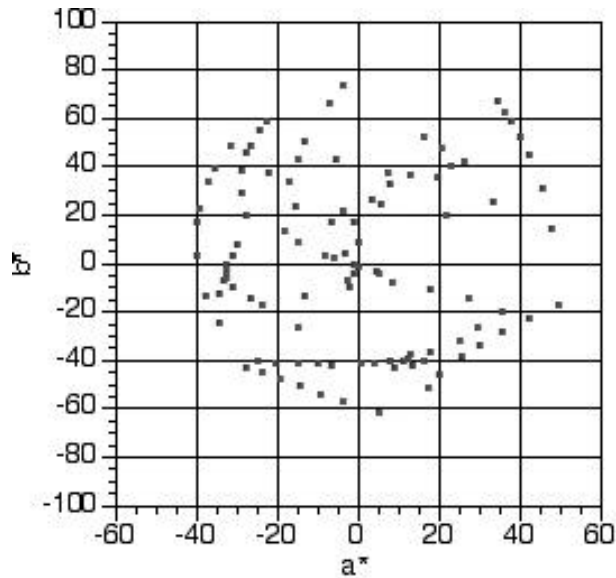


**Figure 6c.** Spectral reflectances of poster-color painted patches (D50 illuminant, 2° observer)

## II) Spectral Analysis

A principal component analysis was performed for the GretagMacbeth ColorChecker and for both painted patches.

Principal component analyses was performed in reflectance space and figures 7a, 7b, and 7c show the plot of the 1<sup>st</sup> to 6<sup>th</sup> eigenvectors of Macbeth ColorChecker, acrylic and poster painted patches, respectively.

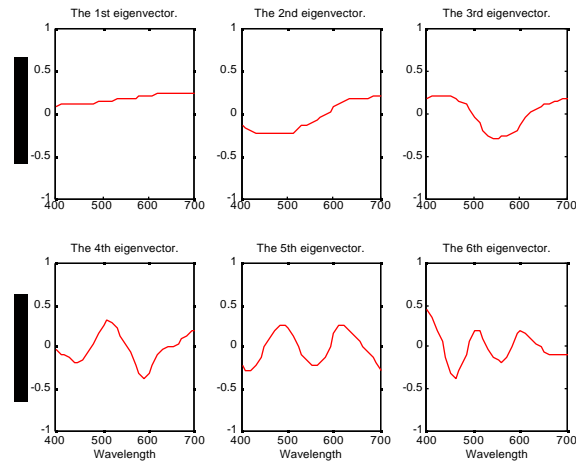


**Figure 7a.** Plot of the first to sixth eigenvectors of GretagMacbeth ColorChecker reflectances.

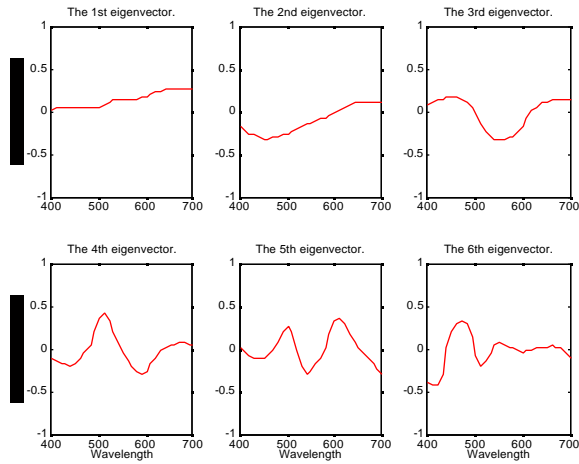


**Figure 7b.** Plot of the first to sixth eigenvectors of acrylic painted patches reflectances.

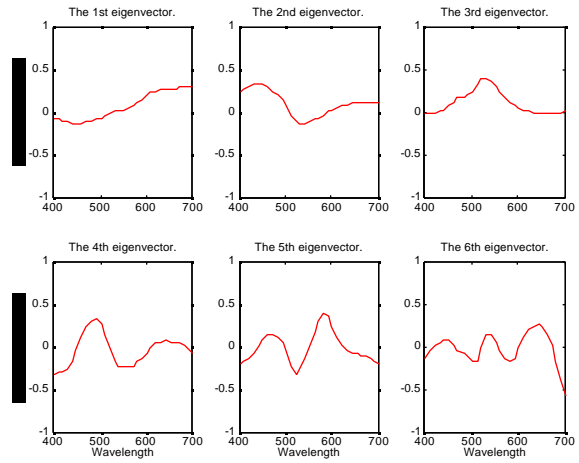


**Figure 7c.** Plot of the first to sixth eigenvectors of poster-color painted patches reflectances.

Comparing Figure 7b and 7c it is possible to observe that the eigenvectors of acrylic and poster-color painted patches reflectances differ from each other. Therefore, the painted patch sets are statistically different as expected.

Table I summarizes the cumulative contribution of the eigenvectors for Macbeth ColorChecker and the sets of painted patches.

**Table I.** Cumulative contribution of the eigenvectors.

Number of eigenvectors	Cumulative Contribution (%) for GretagMachbeth Color Checker	Cumulative Contribution (%) for acrylic painted patches	Cumulative Contribution (%) for poster-color painted patches
1	65.99	65.81	65.18
2	90.14	86.91	88.05
3	98.34	98.50	96.69
4	99.20	99.47	98.60
5	99.66	99.73	99.23
6	99.80	99.83	99.60
7	99.87	99.92	99.86
8	99.94	99.95	99.95
9	99.97	99.98	99.97
10	99.98	99.99	99.98
11	99.99	100.00	99.99
12	100.00	100.00	100.00

Table II shows the influence of the number of eigenvectors on the colorimetric and spectral accuracy of the spectral reconstruction of each patch. The colorimetric accuracy is calculated using CIE94 under D50 and 2° observer. Figures 8a, 8b, and 8c show the histogram of  $E^*_{94}$  between the measured spectral reflectance and the spectral reflectance predicted using 6 eigenvectors for Macbeth ColorChecker, acrylic and poster-color painted patches, respectively.

**Table II.** Influence of the number of eigenvectors used in the spectral reconstruction on the colorimetric and spectral error.

Number of eigenvectors	GretagMachbeth ColorChecker		Acrylic painted patches		Poster-color painted patches	
	Mean $\Delta E^*_{94}$	rms reflectance factor	Mean $\Delta E^*_{94}$	rms reflectance factor	Mean $\Delta E^*_{94}$	rms reflectance factor
1	24.6	0.140	26.58	0.140	45.4	0.181
2	16.8	0.076	15.64	0.068	49.2	0.127
3	3.07	0.032	4.10	0.027	3.08	0.036
4	1.23	0.022	1.28	0.016	1.79	0.019
5	0.67	0.015	0.66	0.012	1.19	0.015
6	0.26	0.013	0.37	0.009	1.03	0.012
7	0.24	0.011	0.32	0.007	0.32	0.006
8	0.13	0.010	0.19	0.005	0.18	0.004
9	0.16	0.007	0.10	0.004	0.08	0.003
10	0.05	0.003	0.05	0.002	0.08	0.003
11	0.02	0.002	0.02	0.001	0.07	0.002
12	0.002	0.002	0.01	0.001	0.06	0.002

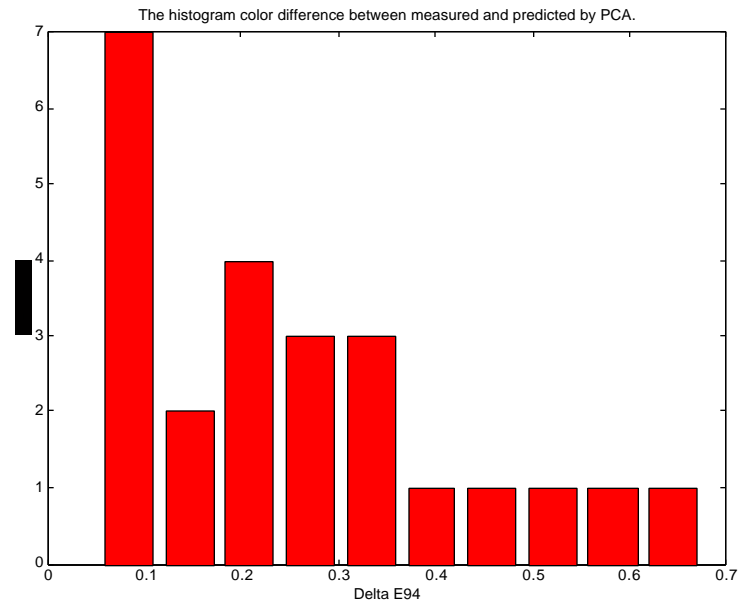


**Figure 8a.**  $E^*_{94}$  histogram for GretagMacbeth ColorChecker reconstructed using 6 eigenvectors.

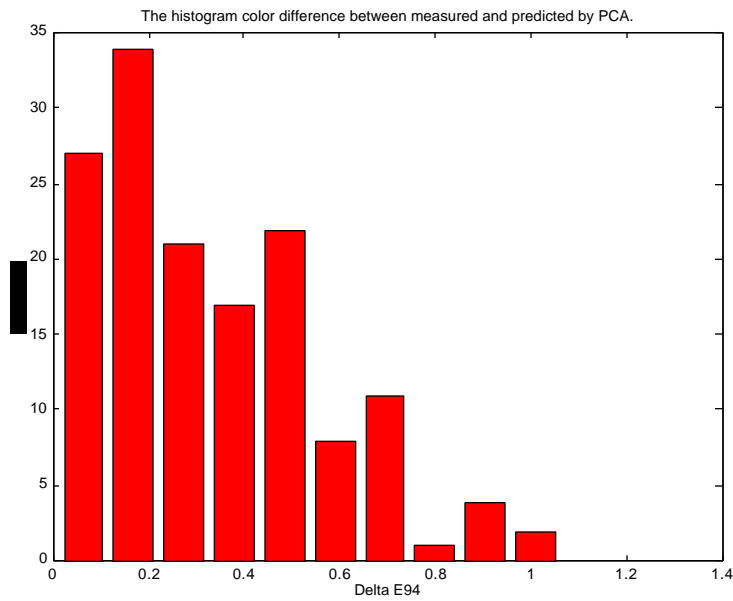


**Figure 8b.**  $E^*_{94}$  histogram for acrylic painted patches reconstructed using 6 eigenvectors.

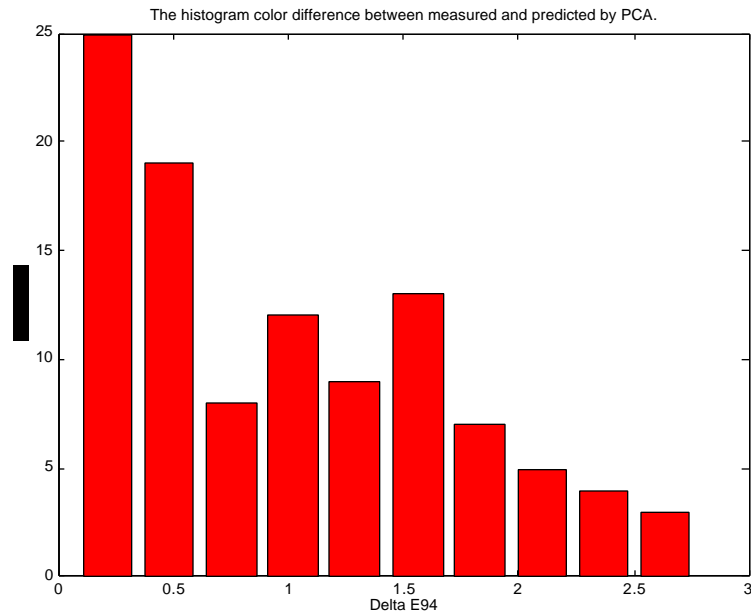


**Figure 8c.**  $E^*_{94}$  histogram for poster-color painted patches reconstructed using 6 eigenvectors.

From the results above, the use of 6 eigenvectors seems to be a comprise between the cost (number of channels) and the accuracy. Using 6 eigenvectors it is possible to reach a theoretical accuracy with average reflectance factor rms error of 1% and unit  $E^*_{94}$

### III) Choice of absorption filter

Various combinations of filters are used to simulate the digital counts of the IBM Pro/3000 digital camera system and estimate the spectral estimation using a transformation matrix from simulated digital counts to the weights of the eigenvectors. Kodak Wratten filters number 38 (light-blue filter), 66 (very-light-green) and a didymium filter whose transmittances are shown in Figure 9 were used to generate the signals. The didymium filter was used to separate the overlap between red and green sensitivities of the digital camera system. The transmittances were measured using the Macbeth ColorEye 7000. The results for the spectral estimation of the GretagMacbeth ColorChecker are shown in Table III. The metameric index was calculated using Fairman metameric black method, between standard illuminant D50 and reference illuminant A using  $E^*_{94}$  in the calculations.

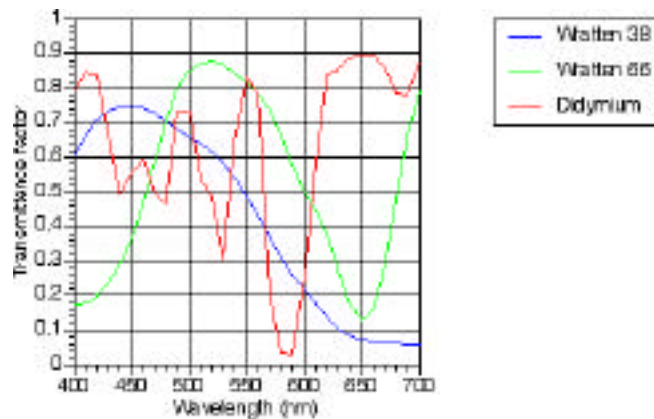


**Figure 9.** Transmittance of two absorption filters and one didymium filter.

**Table III.** Spectral reconstruction of GretagMacbeth ColorChecker rendition chart patches using 6 eigenvectors and 6 simulated digital signals

Patch	$\Delta E^*_{94}$	reflectance factor rms error	Metameric Index
6 eigenvectors and 6 signals: R,G,B without filter and with light-blue absorption filter			
<b>Average</b>	<b>0.4</b>	<b>0.021</b>	<b>0.3</b>
<b>Std Dev</b>	0.3	0.010	0.4
<b>Max</b>	1.1	0.053	1.8
<b>Min</b>	0.04	0.002	0.04
6 eigenvectors and 6 signals: R,G,B without filter and with very-light-green absorption filter			
<b>Average</b>	<b>0.2</b>	<b>0.018</b>	<b>0.2</b>
<b>Std Dev</b>	0.2	0.007	0.2
<b>Max</b>	0.8	0.038	0.9
<b>Min</b>	0.03	0.002	0.01
6 eigenvectors and 6 signals: R,G,B without filter and with didymium filter			
<b>Average</b>	<b>0.5</b>	<b>0.021</b>	<b>0.8</b>
<b>Std Dev</b>	0.4	0.009	0.9
<b>Max</b>	1.4	0.044	3.3
<b>Min</b>	0.05	0.002	0.02
6 eigenvectors and 6 signals: R,G,B with light-blue and with didymium filters			
<b>Average</b>	<b>0.5</b>	<b>0.021</b>	<b>0.5</b>
<b>Std Dev</b>	0.4	0.010	0.5
<b>Max</b>	1.8	0.051	1.8
<b>Min</b>	0.08	0.002	0.01
6 eigenvectors and 6 signals: R,G,B with light-blue and with very-light-green filters			
<b>Average</b>	<b>0.4</b>	<b>0.022</b>	<b>0.2</b>
<b>Std Dev</b>	0.5	0.009	0.2
<b>Max</b>	1.8	0.038	0.8
<b>Min</b>	0.06	0.002	0.02
6 eigenvectors and 6 signals: R,G,B with very-light-green and didymium filters			
<b>Average</b>	<b>0.4</b>	<b>0.019</b>	<b>0.3</b>
<b>Std Dev</b>	0.3	0.008	0.4
<b>Max</b>	1.1	0.037	1.9
<b>Min</b>	0.06	0.002	0.05

The results using simulated digital counts were worse than the theoretical estimation of the spectral reflectance from the eigenvectors presented in Table II for GretagMacbeth ColorChecker using 6 eigenvectors as expected because in the simulated digital counts there is measurement and estimation noise. The various possible combinations of trichromatic signals produced similar spectral and colorimetric performances. It shows that although the spectral reconstruction performance in reflectance space depends on the sample data, the results for different combinations of trichromatic signals were not significantly different. Since we use real signal instead of simulated digital counts the noise introduced by the imaging system will be certainly greater than the accuracy obtained using a certain filter against an optimal filter. Here, I would like to point out that the choice of filter can be critical and the bandwidth should be sufficiently wide and the filter needs to provide signals triplets of signals that are not correlated to another triplet used in the spectral estimation.

#### IV) Comparison between the spectral estimation performance using narrow-band interference filter monochrome multi-spectral acquisition and wide-band absorption trichromatic acquisition

The IBM Pro/3000 Digital Camera System can be switched from monochrome capture to trichromatic capture (using a filter wheel with R, G, B filters and a clear filter) and it makes possible to use the same imaging system to capture both narrow-band (using interference filters and monochromatic mode) and wide-band (using absorption filter and trichromatic mode). For the absorption filter, the Kodak Wratten 38 (light-blue) depicted in Figure 1 was used. For the interference filters six Ealing interference filters shown in Figure 10 are measured using the Macbeth ColorEye 7000 (UV excluded) and the measured transmittance factors are shown in Figure 11.



**Figure 10.** Ealing interference filters used for the narrow-band multi-spectral acquisition.

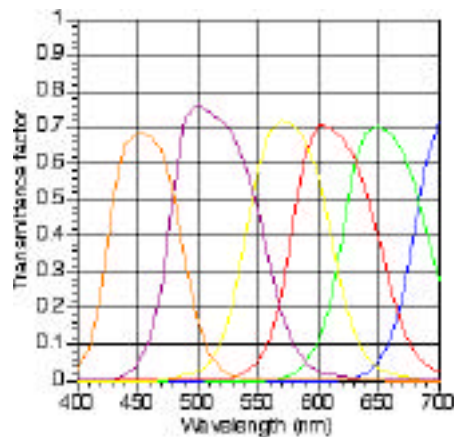


**Figure 11.** Ealing interference transmittance factors in the visible region.

Both interference and absorption filters were held in front of the digital camera head as shown in Figures 12a and 12b, respectively.



**Figure 12a.** IBM digital camera head with red interference filter.

**Figure 12b.** IBM digital camera head with light blue absorption filter.

The results of the spectral estimation are summarized in Table IV. The  $E^*_{94}$  histogram (D50 and 1931 observer) are presented in Figures 13a and 13b.

**Table IV.** Colorimetric and spectral accuracy of GretagMacbeth ColorChecker rendition chart using 6 signals from both narrow-band and wide-band approaches.

Measure	$\Delta E^*_{94}$	reflectance factor rms error	Metameric Index
6 eigenvectors and 6 signals: R,G,B without filter and with light-blue absorption filter			
<b>Average</b>	2.4	0.037	0.6
<b>Std Dev</b>	1.5	0.018	0.4
<b>Max</b>	6.3	0.064	1.6
<b>Min</b>	0.1	0.004	0.0
6 eigenvectors and 6 signals: monochrome camera and interference filters			
<b>Average</b>	2.8	0.031	0.8
<b>Std Dev</b>	1.6	0.012	0.6
<b>Max</b>	6.1	0.053	2.6
<b>Min</b>	0.7	0.005	0.1

It is possible to see from Table IV and Figures 13a and 13b that the wide-band method using absorption filter produced slightly better results than the performance using monochrome camera and interference filters showing the effectiveness of the method. Figure 14a, 14b, 14c and 14d show a the spectral match for the orange yellow and neutral 8 patches of the GretagMacbeth Color Checker using both image acquisition methods. In both cases the method using absorption filters and trichromatic camera presented better results than the method using interference filters and monochromatic camera.

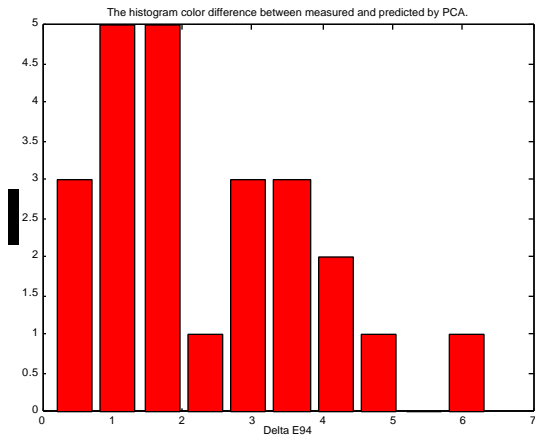


**Figure 13a.**  $E^*_{94}$  (D50 and 1931) between the measured and estimated spectral reflectance using 6 signals obtained combining a trichromatic camera and absorption filter.

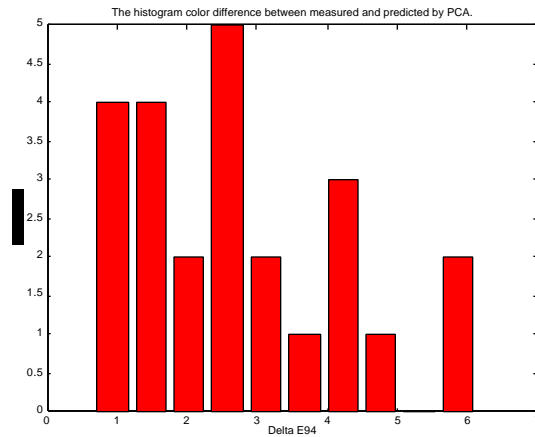
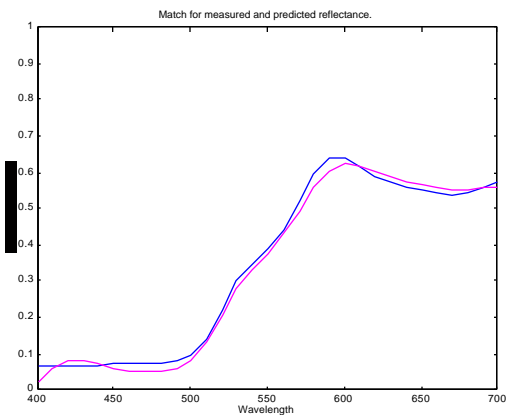
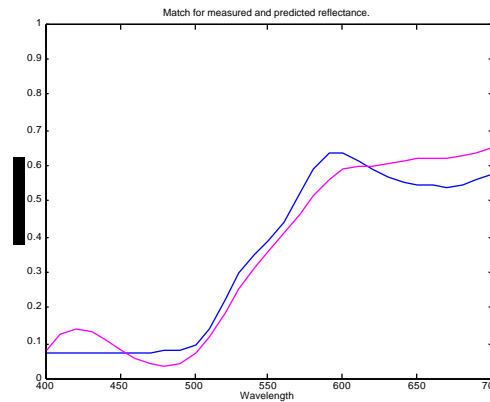


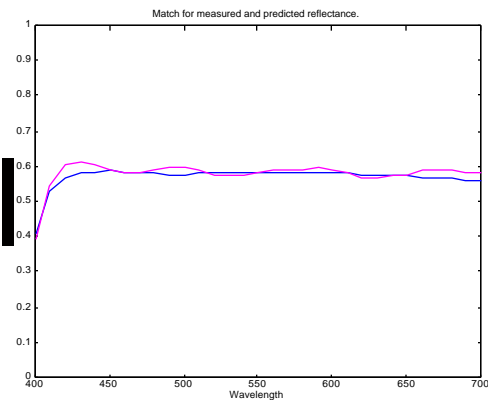
**Figure 13b.**  $E^*_{94}$  (D50 and 1931) between the measured and estimated spectral reflectance using 6 signals obtained combining a monochromatic camera and 6 interference filters.



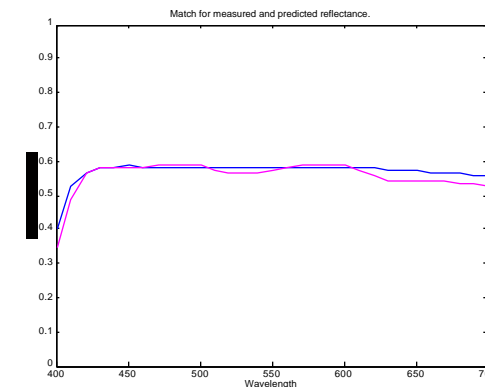
**a** Orange Yellow patch prediction match using absorption filter and trichromatic camera.



**b** Orange Yellow patch prediction match using interference filter and monochromatic camera.



**c** Neutral 8 patch prediction match using absorption filter and trichromatic camera.



**d** Neutral 8 patch prediction match using interference filter and monochromatic camera.

**Figure 14.** Comparison between measured spectral reflectance (blue curve) and estimated spectral reflectance (magenta curve) for two GretagMacbeth ColorChecker patches using two different methods.

**V) Spectral estimation of a target using the eigenvectors derived for a different general target.**

In this experiment a more general oil painting target was considered. This target depicted in Figure 15 was made using cobalt blue, manganese blue, ultramarine blue, Prussian blue, cerulean blue, indanthrone blue, phthalocyanine blue, slate gray, graphite gray, mixture sap green, permanent sap green, phthalocyanine green, phthalocyanine green-yellow, permanent green light, permanent green deep, cadmium green, terre-verte-Gamblin, terre-verte Williamsburg, viridian, cadmium yellow deep, cadmium yellow light, cadmium yellow medium, cadmium yellow pale, basic yellow medium, hansa yellow deep, hansa yellow light, cadmium orange, indian yellow, transparent earth yellow, cadmium vermilion red light, cadmium red, cadmium red light, naphthol red-yellow shade, alizarin crimson, alizarin permanent, burnt sienna-Gamblin, burnt sienna-Williamsburg, transparent earth red, transparent earth orange, Naples yellow hue, Naples Yellow-blockX, Naples yellow, Naples yellow Italian, stilt de grain, yellow ochre, raw sienna, yellow ochre burnt, Italian earth, Permalba white, raw umber-Gamblin, raw umber-Williamsburg, burnt umber, asphaltum, transparent brown, Van Dyke brown, brown madder alizarin, titanium white, replacement blake white, alky white, blue radiant, turquoise radiant, yellow radiant, lemon radiant, green radiant, violet radiant, magenta radiant, and red radiant. The distribution in  $a^* \times b^*$  space of the GretagMacbeth ColorChecker for D50 illuminant and  $2^\circ$  observer is shown in Figure 6.



**Figure 15.** Oil painting target

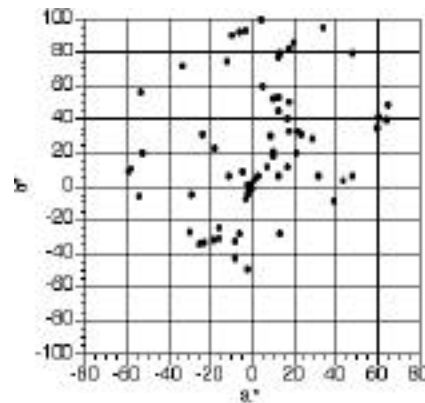


**Figure 16.**  $a^*b^*$  plot for oil painting target (D50 illuminant,  $2^\circ$  observer).

Principal component analyses was performed for the oil painting targets and Figure 17 shows the plot of the 1<sup>st</sup> to 6<sup>th</sup> eigenvectors of the target. Figure 18 shows the histogram of  $E^*_{94}$  (D50, 1931) between the measured spectral reflectance and the spectral reflectance predicted using 6 eigenvectors.

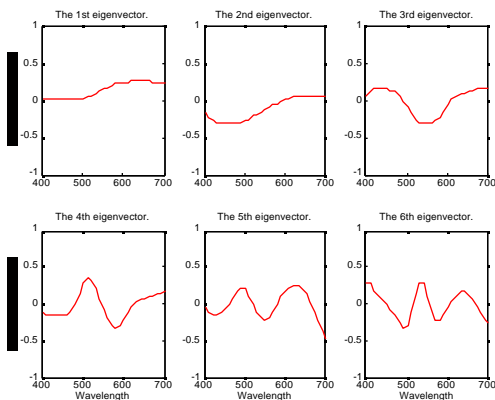


**Figure 17.** Plot of the first to sixth eigenvectors of the oil painting spectral reflectances.

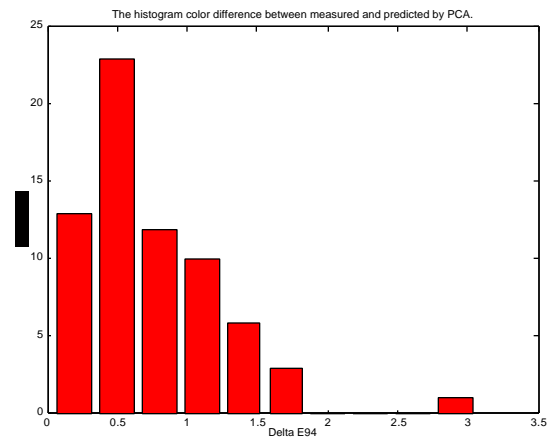


**Figure 18.**  $E^*_{94}$  (D50, 1931) histogram for the oil painting targets reconstructed using 6 oil painting eigenvectors.

In the next step, the eigenvectors of the oil painting target were substituted by the eigenvectors of the GretagMacbeth ColorChecker rendition chart patches reflectances (clearly comparing Figure 7a and 17 we can see that are very similar in shape) and the checker eigenvectors were used to predict theoretically the spectral reflectance curves of the oil painting targets. Figure 19 shows the histogram of  $E^*_{94}$  (D50, 1931) between the measured and predicted spectral reflectances of the oil painting target using 6 checker eigenvectors. Surprisingly the estimation of the oil painting targets using the checker eigenvectors presented a better performance than using the oil painting eigenvectors. I believe that the ColorChecker presents a better spectral distribution than the oil painting targets. And this better distribution has an impact in how the spectral tools like the principal component analysis works. I would like to point out that the ColorChecker was a rendition chart that was scientifically studied while the oil painting target was created by a painter with available pigments.

Table V summarizes the results of the reconstruction of the oil painting targets from its digital counts using oil painting eigenvectors and using checker eigenvectors. Figure 20 and 21 shows the histogram of  $E^*_{94}$  (D50, 1931) between the measured and predicted spectral reflectances from digital counts of the oil painting target using 6 oil painting eigenvectors and 6 checker eigenvectors, respectively.

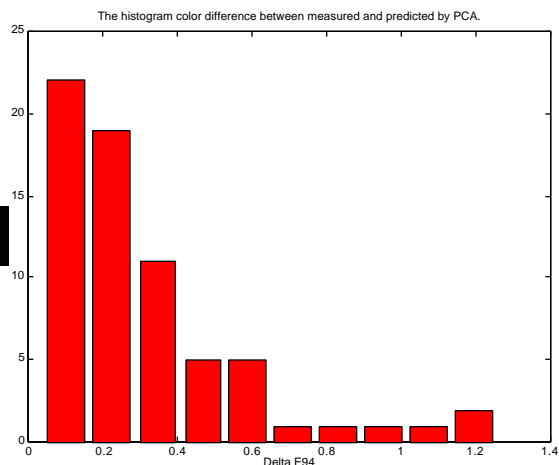


**Figure 19.**  $E^*_{94}$  (D50, 1931) histogram for the oil painting targets reconstructed using 6 oil painting eigenvectors.

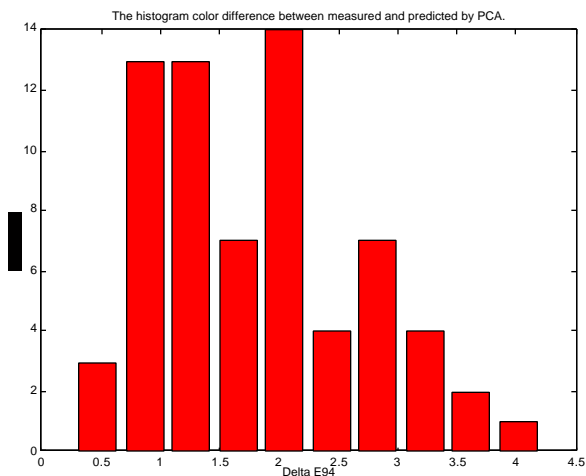


**Figure 20.**  $E^*_{94}$  (D50, 1931) histogram for the oil painting targets reconstructed from digital counts using 6 oil painting eigenvectors.

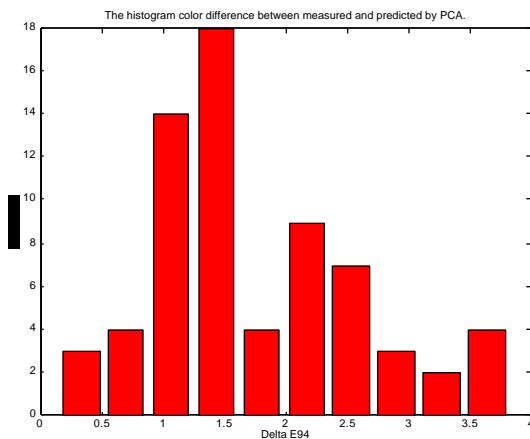
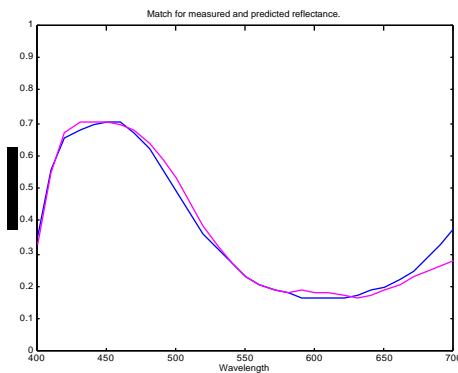


**Figure 21.**  $E^*_{94}$  (D50, 1931) histogram for the oil painting targets reconstructed from digital counts using 6 checker eigenvectors.

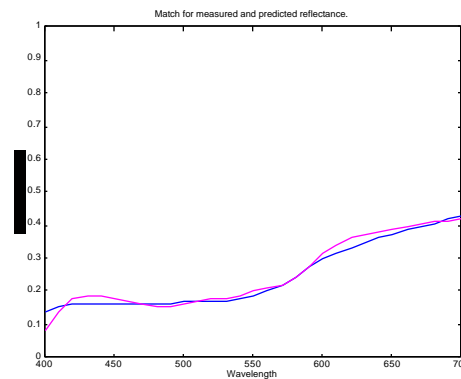
**Table V.** Colorimetric and spectral accuracy of oil painting target spectral estimation using 6 signals (R,G,B without filter and with light-blue absorption filter) using both checker and oil painting eigenvectors.

Measure	$\Delta E^*_{94}$	reflectance factor rms error	Metameric Index
6 eigenvectors and 6 signals and oil painting eigenvectors			
<b>Average</b>	1.8	0.033	0.3
<b>Std Dev</b>	0.9	0.015	0.2
<b>Max</b>	4.2	0.084	1.0
<b>Min</b>	0.3	0.014	0.0
6 eigenvectors and 6 signals and checker eigenvectors			
<b>Average</b>	1.7	0.034	0.3
<b>Std Dev</b>	0.8	0.018	0.2
<b>Max</b>	3.8	0.109	1.2
<b>Min</b>	0.2	0.010	0.0

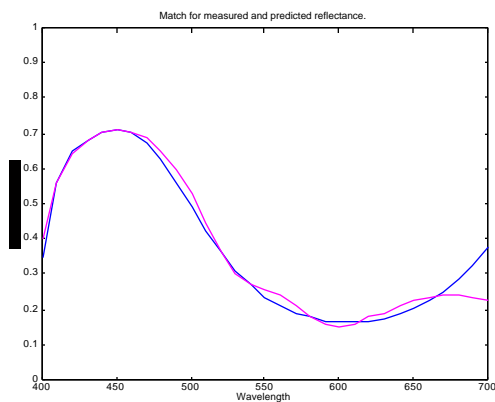
Figures 22a and 22b show some spectral matches for comparing oil painting targets measured reflectance and prediction from digital counts using eigenvectors derived for the oil painting target spectral reflectances. Figures 22c and 22d show some spectral matches for comparing oil painting targets measured reflectance and prediction from digital counts using eigenvectors derived for the ColorChecker spectral reflectances.



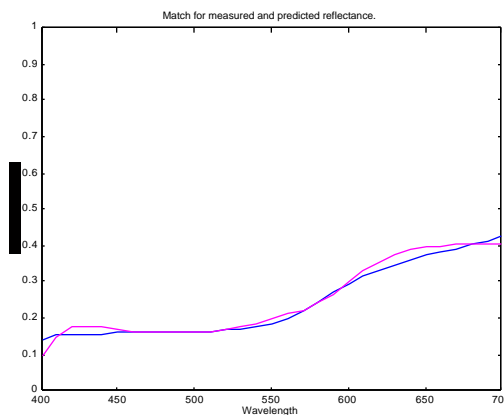
**a** Ultramarine blue patch prediction match using oil painting eigenvectors



**b** Burnt Sienna, Williamsburg patch prediction match using oil painting eigenvectors.



**c** Ultramarine blue patch prediction match using checker eigenvectors.



**d** Burnt Sienna, Williamsburg patch prediction match using oil checker eigenvectors.

**Figure 22.** Comparison between measured spectral reflectance (blue curve) and estimated spectral reflectance (magenta curve) for two oil painting patches using two different set of eigenvectors.

From Table V and Figures 20, 21 and 22 it is possible to conclude that the eigenvectors of the ColorChecker can be used to reconstruct the spectral reflectances of the oil painting target.

## Discussions

In this report it was shown that the new approach using trichromatic digital camera and absorption filters was equivalent or even better in terms of accuracy compared to the spectral acquisition approach using monochrome camera and interference filters. This new approach also has the advantage of avoiding inherent problems related to the use of interference narrow-band filters. This new wide-band approach using absorption filters reply on *a priori* analysis of representative sample of the imaging target. Although more future work is still necessary to corroborate our present results, this report also showed encouraging evidences that make possible to design a universal target to derive the eigenvectors that are necessary for the spectral estimation. It will be fundamental for the cases in which we do not know the spectral characteristic of the pigments.

## References

- 1.Saunders, D., Cupitt, J., *Image processing at the National Gallery: The VASARI Project*, National Gallery technical bulletin, **14**:72 (1993).
- 2.Berns, R. S., Challenges for color science in multimedia imaging, *Proc. CIM'98 Colour Imaging in Multimedia*, University of Derby, 123-133 (1998).
- 3.Hardeberg, J. Y., Schmitt, F., Brettel, H., Crettez, J-P. and Maitre, H., Multispectral imaging in multimedia, *Proc. CIM'98 Colour Imaging in Multimedia*, University of Derby, 75-86 (1998).
- 4.Maitre, H., Schmitt, F. J. M., Crettez, J.-P., Wu, Y., Hardeberg, J. Y., Spectrophotometric image analysis of fine art paintings, *Proc. IS&T/SID Fourth Color Imaging Conference: Color Science, Systems and Applications*, 50-53 (1996).
- 5.Haneishi, H., Hasegawa, T., Tsumura, N., Miyake, Y., Design of color filters for recording artworks, *IS&T's 50th Annual Conference*, 369-372 (1997).
- 6.Miyake, Y., Yokoyama, Y., Obtaining and reproduction of accurate color images based on human perception, *Proc. SPIE 3300*: 190 (1998).
- 7.König, F., Präfke, W., A multispectral scanner, *Proc. CIM'98 Colour Imaging in Multimedia*, University of Derby, 63-73 (1998).
- 8.Vent, D. S. S., *Multichannel analysis of object-color spectra*, Master Degree Thesis, R.I.T., 1994.
- 9.Burns, P. D., *Analysis of image noise in multi-spectral color acquisition*, Ph.D. Thesis, R.I.T., 1997.
- 10.König, F., Präfke, W., The practice of multispectral image acquisition, in *International symposium on electronic capture and publishing*, *Proc. SPIE 3409* (1998).
11. F. H. Imai, Multi-spectral Image Acquisition and Spectral Reconstruction using a Trichromatic Digital Camera System associated with absorption filters, Munsell Color Science Laboratory Technical Report, Rochester, NY, 1998, <http://www.cis.rit.edu/research/mcsl/pubs/PDFs/CameraReport.pdf>.
- 12.Pro/3000 Digital Imaging System PISA95 Operator's Manual Version 6.0, IBM, 1996.
- 13.Pro/3000 Digital Imaging System Reference Guide, IBM, 1996.
- 14.Kodak Filters for scientific and technical uses, Data Book, Kodak, Third Edition, 1981.
- 15.Burns, P. D., *Analysis of image noise in multi-spectral color acquisition*, Ph.D. Thesis, R.I.T., 1997.
- 16.Vrhel, M. J., Trussel, H. J., Color correction using principal components, *Color Res. Appl.* **17**: 26 (1992).

17. Präfke, W., Keusen, T., Optimized basis functions for coding reflectance spectra minimizing the visual color difference, *Proc. IS&T/SID 1995 Color Imaging Conference: Color Science, Systems and Applications*, 37-40 (1995).
18. Vrhel, M. J., Gershon, R., Iwan, L. S., Measurement and analysis of object reflectance spectra, *Color Res. Appl.* **19**:4 (1994).
19. Burns, P. D., Berns, R. S., Analysis multispectral image capture, *Proc. IS&T/SID 1995 Color Imaging Conference: Color Science, Systems and Applications*, 19-22 (1996).